Chemical Science

EDGE ARTICLE

View Article Online
View Journal | View Issue

Cite this: *Chem. Sci.*, 2019, **10**, 2153

All publication charges for this article have been paid for by the Royal Society of Chemistry

Received 3rd November 2018
Accepted 15th December 2018

DOI: 10.1039/c8sc04906h

rsc.li/chemical-science

Crystallographic identification of Eu@C_{2n} ($2n$ = 88, 86 and 84): completing a transformation map for existing metallofullerenes†

Lipiao Bao, Pengyuan Yu, Changwang Pan, Wangqiang Shen and Xing Lu *

Revealing the transformation routes among existing fullerene isomers is key to understanding the formation mechanism of fullerenes which is still unclear now because of the absence of typical key links. Herein, we have crystallographically identified four new fullerene cages, namely, C_2(27)-C_{88}, C_1(7)-C_{86}, C_2(13)-C_{84} and C_2(11)-C_{84}, in the form of Eu@C_{2n}, which are important links to complete a transformation map that contains as many as 98% (176 compounds in total) of the reported metallofullerenes with clear cage structures (C_{2n}, $2n$ = 86–74). Importantly, the mutual transformations between the metallofullerene isomers included in the map require only one or two well-established steps (Stone–Wales transformation and/or C_2 insertion/extrusion). Moreover, structural analysis demonstrates that the unique C_2(27)-C_{88} cage may serve as a key point in the map and is directly transformable from a graphene fragment. Thus, our work provides important insights into the formation mechanism of fullerenes.

Introduction

Fullerenes are a collection of spherical pure-carbon molecules consisting of exactly 12 pentagons and a variable number of hexagons.[1] Although C_{60} and C_{70} are abundantly produced and have received extensive attention,[2] pure isomers of higher fullerenes (C_{2n}, $2n > 70$) are rarely reported because of their low solubility in organic solvents and the tremendous number of possible isomers that may exist in reality.[3] Alternatively, endohedral metal-doping has had great success in stabilizing higher fullerenes to produce a new family of hybrid molecules named endohedral metallofullerenes (EMFs).[4,5] Up to now, hundreds of EMF-isomers have been isolated and structurally characterized.[4–7] Their cage sizes range from C_{60} to even C_{108} and the metallic species are also diverse and can be one or two pure metal atoms or a cluster of metal carbides, nitrides, oxides, sulfides and even cyanides.[4–7] It is noteworthy that although many possible cage structures are available for a given C_{2n},[3] the experimentally obtained species are limited to a small number of compounds.[4–7] For instance, as many as seven isomers that obey the 'isolated pentagon rule' (IPR)[8] are available for C_{80},[3] but only the I_h-C_{80} and D_{5h}-C_{80} cages have been found for M_3N@C_{80},[4,9–11] and C_{2v}(5)-C_{80} has been found for Sc_2C_2@C_{80}.[12,13]

It is certainly of special interest to understand the inter-cage transformation between isolated fullerene/EMF isomers which is key to clarifying the formation mechanism of fullerenes. In the very beginning of fullerene research, the structural transition from C_{60} to C_{70} was described like this: C_{60} is cut in half, and one half is rotated by 36 degrees relative to the other, and then a 10-carbon ring is added in between, and thus C_{70} forms.[14] Obviously, this route is too complicated to happen in reality. In fact, both theoretical and experimental results suggest that the transformations between fullerene isomers may involve merely two processes: Stone–Wales transformation (SWT)[15] and C_2-extrusion or insertion (Fig. 1). Theoretical calculations suggest that the energy barrier of such facile transformations might be

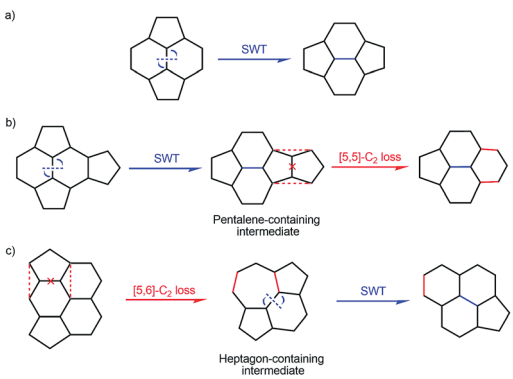

Fig. 1 Transformation pathways of fullerenes involving (a) one SWT, (b) one SWT and one subsequent [5,5]-C_2 extrusion or (c) one [5,6]-C_2 elimination and one subsequent SWT. For the ease of explanation, we follow a top-down manner in the figure and context.

State Key Laboratory of Materials Processing and Die & Mould Technology, School of Materials Science and Engineering, Huazhong University of Science and Technology, 1037 Luoyu Road, Wuhan, 430074, China. E-mail: lux@hust.edu.cn

† Electronic supplementary information (ESI) available: Spectroscopic results, crystal structures, metallofullerenes included in the transformation map, and transformation routes. CCDC 1578319–1578322. For ESI and crystallographic data in CIF or other electronic format see DOI: 10.1039/c8sc04906h

easily overcome in the very hot environments of fullerene formation[16] and the reported transformation reactions are favored in terms of entropy.[17] The proposed SWT and C_2 elimination/addition could generate labile pentalene/heptagon containing intermediates, which has been demonstrated by the experimental identification of heptagon[18,19] and fused-pentagon[20–26] containing metallofullerenes with the endohedral metallic unit or exohedral functionalized moieties[27–29] as stabilizers.

During recent years, more and more higher-fullerene cages have been captured and structurally identified, mainly in the form of EMFs which enables in-depth investigation of the inter-cage transformations among existing fullerene cages.[4,5] For example, Balch and co-workers identified $Sc_2S@C_s(6)$-C_{82} and $Sc_2S@C_{3v}(8)$-C_{82} and proposed the interconversion process between $C_s(6)$-C_{82} and $C_{3v}(8)$-C_{82} through two SWTs[30] with the commonly encountered $C_{2v}(9)$-C_{82} as the intermediate. In another work, they found that four $Sm@C_{90}$ isomers can be related pairwise to one another through sequential SWTs.[31] Besides, Feng *et al.* revealed that $Sc_2O@C_{2v}(3)$-C_{78} and $Sc_2O@D_{3h}(5)$-C_{78} are closely related *via* a single SWT transformation.[32] A more brilliant study was from Dorn and co-workers who captured and identified $M_2C_2@C_1(51383)$-C_{84} (M = Y and Gd) which can transform into the other seven smaller cages, namely $C_1(51383)$-C_{84}, $C_{3v}(8)$-C_{82}, $C_{2v}(9)$-C_{82}, $C_s(6)$-C_{82}, $C_s(39663)$-C_{82}, $I_h(7)$-C_{80} and $D_{5h}(6)$-C_{80}, implying a 'top-down formation mechanism' for fullerenes.[26] In that report, the authors also provided concrete mass spectrometric results to confirm that the formation route of empty fullerenes is the same as that of EMFs.[26] Recently, our group reported that the defective $C_2(816)$-C_{104} cage can change to the other three ideal cages, namely $D_5(450)$-C_{100}, $C_s(574)$-C_{102} and $D_{3d}(822)$-C_{104}, *via* multiple SWTs and C_2-extrusion.[33] It is clear that the transformation scheme of existing fullerenes/EMFs is rather fragmentary with the entire map remaining far from complete.

Herein, we have made a solid step towards completing the transformation map of existing metallofullerenes by capturing four key cages, namely, $C_2(27)$-C_{88}, $C_1(7)$-C_{86}, $C_2(13)$-C_{84} and $C_2(11)$-C_{84} in the form of europium-containing metallofullerenes. These four cages are key links in the map that covers up to 98% of known metallofullerenes with a C_{2n} ($2n$ = 74–86) cage through very facile transformation routes. In addition, we propose that $C_2(27)$-C_{88} is a starting point of the map, and is not obtainable from any of the existing C_{90} isomers through facile steps, but is a possible product of self-assembly of a graphene fragment.

Results and discussion

Soot containing europium metallofullerenes was synthesized by vaporizing graphite rods containing a mixture of Eu_2O_3 and graphite powder (molar ratio of Eu/C = 1 : 50) under 300 mbar helium in an arc-discharge chamber. The soot was collected and extracted with carbon disulfide. Upon solvent removal, the crude mixture was redissolved in toluene and subjected to multi-stage high performance liquid chromatographic (HPLC) separation (Fig. S1†). The purity of the isolated $Eu@C_{2n}$ ($2n$ = 88, 86 and 84) isomers is confirmed by both HPLC (Fig. 2a) and laser desorption/ionization time-of-flight (LDI-TOF) mass spectroscopic analyses (Fig. 2b). The vis-NIR absorption spectra of the four compounds are shown in Fig. 3. All show obvious absorptions in the range from 400 to 2000 nm with relatively large onsets, suggesting small optical bandgaps (<1.0 eV) and correspondingly low thermodynamic stability. More details are listed in Fig. S2 and Table S1.†

The molecular structures of the four europium-containing metallofullerenes are unambiguously determined by X-ray crystallography as $Eu@C_2(27)$-C_{88}, $Eu@C_1(7)$-C_{86}, $Eu@C_2(13)$-C_{84} and $Eu@C_2(11)$-C_{84}. Notably, this is the first crystallographic identification of europium-containing EMFs since they were first reported over two decades ago.[34] More significantly, the $C_2(27)$-C_{88} and $C_1(7)$-C_{86} cages are unprecedented even without theoretical prediction.

Fig. 4 shows the molecular structures of these four endohedrals co-crystallized with Ni^{II}(OEP) (OEP is the dianion of octaethylporphyrin). The porphyrin moiety faces a relatively flat region of each cage with the shortest Ni-to-cage-carbon distances ranging from 2.825 to 2.926 Å, indicative of π–π interactions. In the case of $Eu@C_2(27)$-C_{88} and $Eu@C_1(7)$-C_{86},

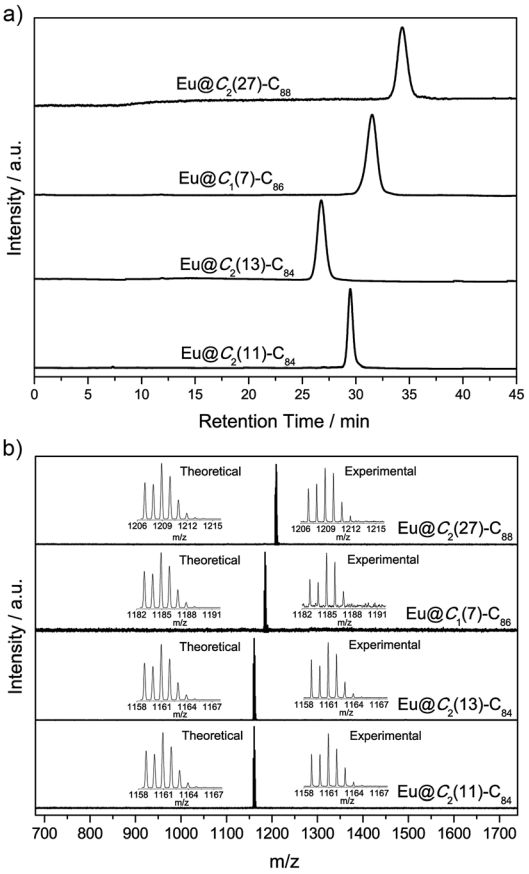

Fig. 2 (a) HPLC chromatograms and (b) LDI-TOF mass spectra of purified $Eu@C_2(27)$-C_{88}, $Eu@C_1(7)$-C_{86}, $Eu@C_2(13)$-C_{84} and $Eu@C_2(11)$-C_{84}. HPLC conditions: Buckyprep column (φ = 4.6 × 250 mm); eluent, toluene; flow rate, 1.0 mL min^{-1}; detection wavelength, 330 nm; r.t. Insets show the theoretical and experimental isotopic distributions of the corresponding metallofullerenes.

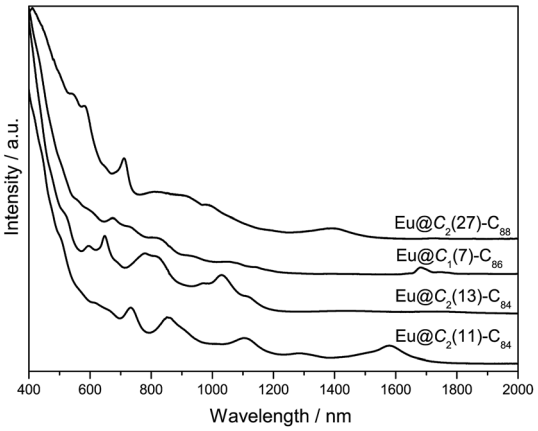

Fig. 3 Vis-NIR absorption spectra of Eu@C_2(27)-C_{88}, Eu@C_1(7)-C_{86}, Eu@C_2(13)-C_{84} and Eu@C_2(11)-C_{84} dissolved in CS_2. The curves are vertically shifted for the ease of comparison.

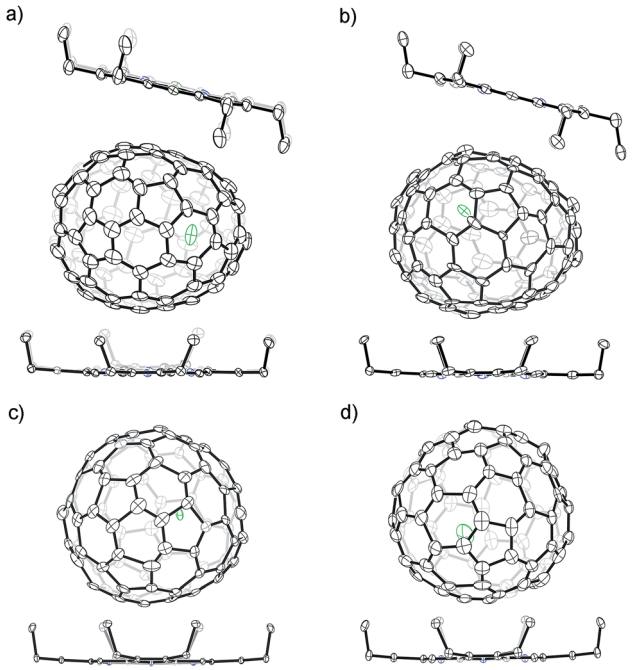

Fig. 4 Ortep drawings of (a) Eu@C_2(27)-C_{88}, (b) Eu@C_1(7)-C_{86}, (c) Eu@C_2(13)-C_{84} and (d) Eu@C_2(11)-C_{84} with thermal ellipsoids set at a 20% probability level. Only one cage orientation and the major metal sites are shown. Solvent molecules, the minor metal sites and H atoms are omitted for clarity.

each fullerene cage is surrounded by two nonparallel Ni^{II}(OEP) molecules in a sandwich-like arrangement and the ethyl groups of one Ni^{II}(OEP) molecule face towards opposite sides to enhance the π–π interactions. In contrast, only one Ni(OEP) molecule is required to assist in the crystallization of the smaller Eu@C_2(13)-C_{84} or Eu@C_2(11)-C_{84} molecules. These results demonstrate that the stacking mode in the co-crystals depends on the shape and size of the endohedral. The Eu atom in each compound shows some degree of disorder (Fig. S3†), suggesting a motional behavior.

Based on these four new cages, we are now able to complete a transformation map of existing metallofullerenes which includes up to 98% of the reported metallofullerenes (metal@C_{2n}, $2n$ = 74–86) with clear cage structures (176 compounds in total; see Table S2† for details). More importantly, the inter-cage transformations require only one or two well-established steps (Stone–Wales transformation or C_2 extrusion/insertion). Note that the transformation map matches with both the bottom-up and top-down formation mechanisms. For the ease of explanation, we follow a top-down manner in the map and context.

Fig. 5 depicts the transformation map and the detailed pathways are illustrated in the ESI (Fig. S4–S41).† The transformation from C_2(27)-C_{88} to C_1(7)-C_{86} is straightforward by a direct [5,6]-C_2 loss and a subsequent SWT. Then a [5,6]-C_2 loss and a SWT on C_1(7)-C_{86} generate C_2(13)-C_{84}. A SWT on C_2(13)-C_{84} affords C_1(12)-C_{84} and a further SWT on the latter produces C_2(11)-C_{84}. Two SWTs convert C_2(11)-C_{84} and C_1(12)-C_{84} into D_{3d}(19)-C_{84} and D_{2d}(23)-C_{84}, respectively. Elimination of a C_2-unit from a pentalene unit generated by a SWT on C_1(7)-C_{86} produces the non-IPR missing link C_1(51383)-C_{84}.[26] A subsequent SWT on C_1(51383)-C_{84} gives another non-IPR C_s(51365)-C_{84}.[26]

The transformations from C_{84} to C_{82} and the isomerization between C_{82} cages are rather clear. A [5,6]-C_2 loss with a subsequent SWT on C_2(13)-C_{84} produces C_2(5)-C_{82} while a SWT with a [5,5]-C_2 loss converts C_2(13)-C_{84}, C_1(12)-C_{84} and C_2(11)-C_{84} into C_{3v}(8)-C_{82}, C_{2v}(9)-C_{82} and C_s(6)-C_{82}, respectively. Alternatively, elimination of the remaining pentalene unit on C_1(51383)-C_{84} and C_1(51365)-C_{84} affords C_s(6)-C_{82} and C_{2v}(9)-C_{82}, respectively.[26] A [5,6]-C_2 extrusion plus an additional SWT on C_1(51383)-C_{84} generates the non-IPR C_s(39663)-C_{82} as well as C_{3v}(8)-C_{82} which are related with a single SWT.[26]

Furthermore, C_{2v}(5)-C_{80} is obtainable *via* one SWT and one subsequent [5,5]-C_2 extrusion from either C_2(5)-C_{82} or C_{3v}(7)-C_{82}, while D_{5h}(6)-C_{80} is generated from C_s(6)-C_{82} through a [5,6]-C_2 loss and a subsequent SWT or from C_s(39663)-C_{82} *via* merely a [5,5]-C_2 elimination.[26] Besides, the C_{3v}(8)-C_{82} cage can shrink into the popular I_h(7)-C_{80} cage *via* a [5,6]-C_2 loss plus a SWT[26] or into the heptagon-containing C_s(hept)-C_{80} cage[18] *via* merely a [5,6]-C_2 extrusion. Structural transformation can also be demonstrated among three isomeric C_{80} cages (D_{5h}(6)-C_{80}, C_{2v}(5)-C_{80} and C_{2v}(3)-C_{80}) *via* merely one SWT.

In further steps, C_{80} can shrink to smaller fullerene cages such as C_{78}, C_{76} and C_{74}. A SWT plus a [5,5]-C_2 loss converts C_{2v}(5)-C_{80}, C_{2v}(3)-C_{80} and I_h(7)-C_{80} into D_{3h}(5)-C_{78}, C_{2v}(3)-C_{78} and C_2(22010)-C_{78}, respectively. Alternatively, the non-IPR C_2(22010)-C_{78} is also obtainable from C_s(hept)-C_{80} *via* a [5,5]-C_2 loss. The transformation between D_{3h}(5)-C_{78} and C_{2v}(3)-C_{78} can be realized by only one SWT.[32] Furthermore, T_d(2)-C_{76} and the non-IPR C_{2v}(19138)-C_{76} are formed with D_{3h}(5)-C_{78} (ref. 32) and C_{2v}(3)-C_{78} as their respective precursors through a SWT plus a [5,5]-C_2 elimination. Both T_d(2)-C_{76} and C_{2v}(19138)-C_{76} can transform into D_{3h}(1)-C_{74} *via* a SWT and a [5,5]-C_2 extrusion. Thus, the transformations among up to 98% of the identified C_{2n} ($2n$ = 86–74) cages employed by EMFs have been uncovered with the inter-cage transformations involving merely one or two well-established steps (Fig. 1). Depending on the encapsulated

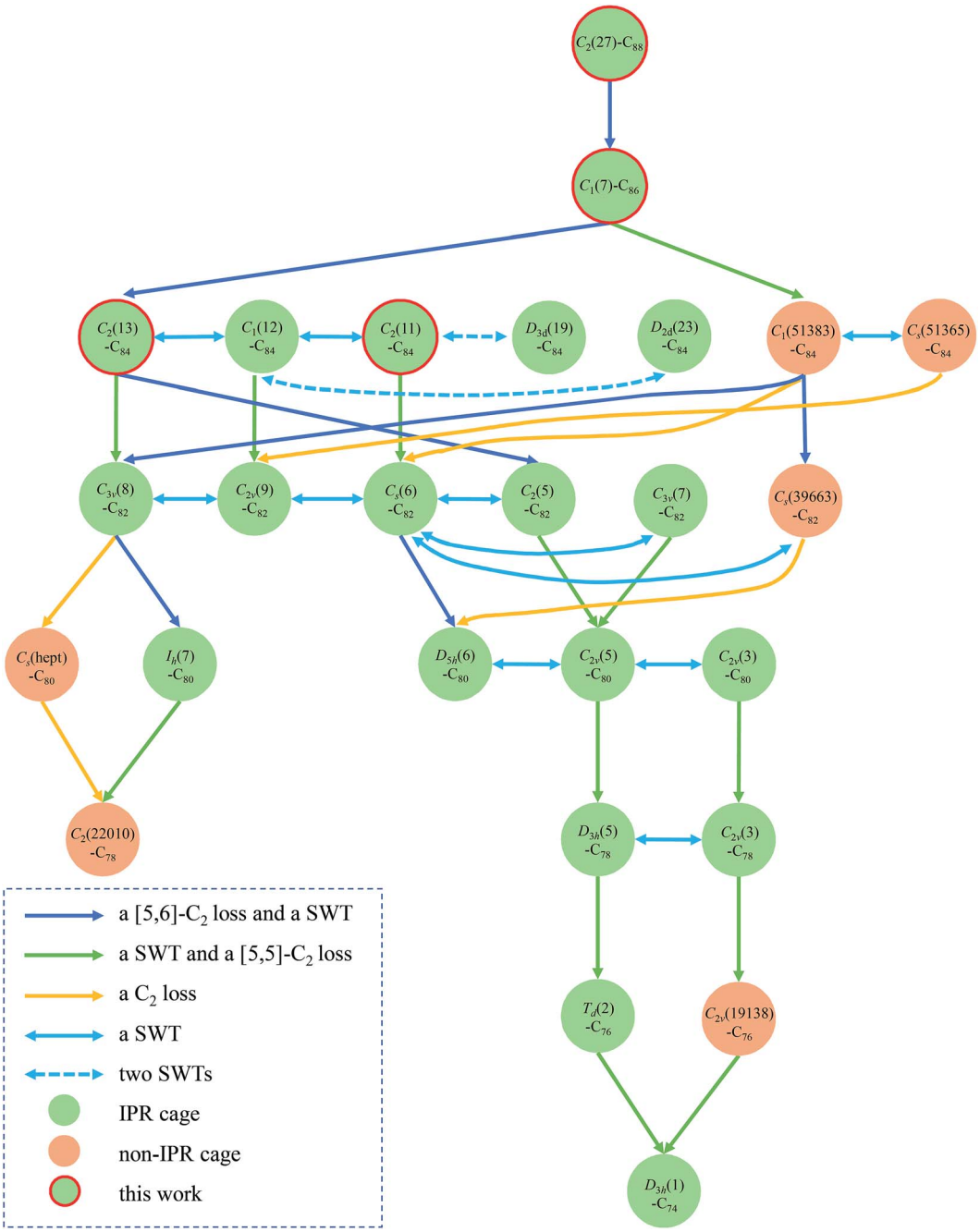

Fig. 5 Transformations among existing metallofullerenes with C_2(27)-C_{88} as the starting top point. As many as 98% of metallofullerenes from C_{86} to C_{74} with known structures are included in the map. The rearrangement pathways involve one or two well-established steps. IPR cages are marked in green and non-IPR cages are marked in yellow. The cages reported in this work are highlighted with red circles. The blue one-way arrow indicates a [5,6]-C_2 loss with a subsequent SWT while the green one-way arrow refers to a SWT followed by a [5,5]-C_2 loss. The yellow one-way arrow corresponds to merely one C_2 loss while the aqua blue two-way arrow indicates a SWT and the dashed aqua blue two-way arrow refers to two SWTs. The detailed transformation pathways are illustrated in the ESI (Fig. S4–S41).†

species, different transformation routes can be expected.[26] However, it should also be mentioned that the encaged metallic unit may change during the transformation process. For example, Y_2@C_{84} is shown to encapsulate a C_2 unit inside the cage to form Y_2C_2@C_{3v}(8)-C_{82}.[35]

One may think that the top C_2(27)-C_{88} cage is possibly converted from a C_{90} cage. However, although as many as six isomeric C_{90} cages (C_1(21)-C_{90}, C_2(40)-C_{90}, C_2(42)-C_{90}, C_2(45)-C_{90}, C_{2v}(46)-C_{90} and C_2(41)-C_{90}) have been identified in the form of EMFs,[31,36–38] none of them could transform into the C_2(27)-C_{88} cage *via* the defined facile routes (Fig. 1). However, our topological analysis reveals that the C_2(27)-C_{88} cage may be directly obtained by the self-assembly of a graphene fragment (Fig. 6), indicating the top-down formation process of fullerenes.

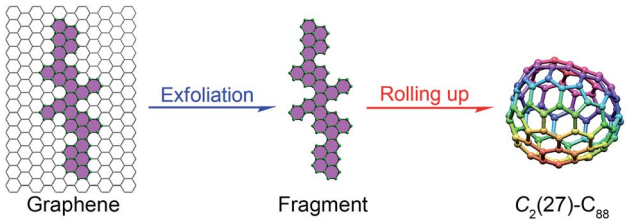

Fig. 6 Proposed formation of $C_2(27)$-C_{88} *via* self-assembly of a graphene fragment.

Another argument for the unique role of the C_{88} cage is the templating effect of Nd_3N leading to the formation of $M_3N@C_{88}$, while the smaller Sc_3N and the larger La_3N clusters adopt the C_{80} and C_{96} cages, respectively.[9,39,40] This interesting C_8 interval (C_{96}–C_{88}–C_{80}) phenomenon is further corroborated by the fact that the defective $C_2(816)$-C_{104} cage (obtained in the form of $La_2C_2@C_2(816)$-C_{104}) can change to the other three ideal cages, namely $D_5(450)$-C_{100}, $C_s(574)$-C_{102} and $D_{3d}(822)$-C_{104} *via* facile routes.[33] Accordingly, we propose that the C_8 interval may play an important role in determining the starting points of metallofullerene transformation. In this regard, the missing transformation between C_{74} and C_{72} in the map can be understood by considering a C_8 interval between C_{80} and C_{72}, which implies that C_{72} may be included in a different map. We acknowledge that the experimentally observed $C_{2v}(9)$-C_{86}, $D_3(19)$-C_{86}, $D_2(35)$-C_{88} and C_s(hept)-C_{88} are not included in our map, which might be a sign of the presence of other transformation routes[19] and hence uncovering new transformation links is still of vital importance.

Conclusions

In summary, we have captured and crystallographically identified four fullerene cages, namely, $C_2(27)$-C_{88}, $C_1(7)$-C_{86}, $C_2(13)$-C_{84} and $C_2(11)$-C_{84}, in the form of europium-containing metallofullerenes. With their accession, a transformation map covering as many as 98% of the experimentally identified EMFs with clear C_{2n} ($2n$ = 86–74) cage structures is presented, in which the inter-cage transformations are limited to merely one or two very favorable steps. Structural analysis demonstrates that the unique $C_2(27)$-C_{88} cage may serve as the key point in the map and is directly transformable from a graphene fragment. Completing the transformation map is key to solving the long-standing puzzle of fullerene formation and could shed light on the construction and applications of novel nano-carbon molecules.

Experimental

Raw soot containing europium-metallofullerenes was synthesized by a direct-arc discharge method and extracted with carbon disulfide. After solvent removal, the mixture was dissolved in toluene and subjected to multi-stage high performance liquid chromatographic (HPLC) separation which gave the desired compounds (Fig. S1†).

Black crystals were obtained by slow diffusion of a benzene solution of Ni^{II}(OEP) into a carbon disulfide solution of each metallofullerene over four weeks. Single-crystal X-ray data were collected at 100 K using synchrotron radiation (0.65250 Å) with a MarCCD detector at beamline BL17B of the Shanghai Synchrotron Radiation Facility. A multi-scan method (SADABS) was used for absorption corrections. The structures were solved with direct methods and were refined with SHELXL-2016.[41]

Conflicts of interest

There are no conflicts to declare.

Acknowledgements

Financial support from the NSFC (No. 51472095 and 51672093) is gratefully acknowledged. We acknowledge the staff at the BL17B beamline of the National Center for Protein Sciences Shanghai (NCPSS) at the Shanghai Synchrotron Radiation Facility for assistance during data collection, and the Analytical and Testing Center in the Huazhong University of Science and Technology for all related measurements.

Notes and references

1 H. W. Kroto, J. R. Heath, S. C. Obrien, R. F. Curl and R. E. Smalley, *Nature*, 1985, **318**, 162–163.
2 K. M. Kadish and R. Ruoff, *Fullerenes: Chemistry, Physics, and Technology*, Wiley-VCH, New York, 2000.
3 P. W. Fowler and D. E. Manolopoulos, *An Atlas of Fullerenes*, Dover Publications, Clarendon, 2007.
4 A. Popov, S. Yang and L. Dunsch, *Chem. Rev.*, 2013, **113**, 5989–6113.
5 X. Lu, L. Echegoyen, A. L. Balch, S. Nagase and T. Akasaka, *Endohedral Metallofullerenes: Basics and Applications*, CRC Press, 2014.
6 S. Yang, T. Wei and F. Jin, *Chem. Soc. Rev.*, 2017, **46**, 5005–5058.
7 X. Lu, L. Feng, T. Akasaka and S. Nagase, *Chem. Soc. Rev.*, 2012, **41**, 7723–7760.
8 H. W. Kroto, *Nature*, 1987, **329**, 529–531.
9 S. Stevenson, G. Rice, T. Glass, K. Harich, F. Cromer, M. R. Jordan, J. Craft, E. Hadju, R. Bible, M. M. Olmstead, K. Maitra, A. J. Fisher, A. L. Balch and H. C. Dorn, *Nature*, 1999, **401**, 55–57.
10 J. C. Duchamp, A. Demortier, K. R. Fletcher, D. Dorn, E. B. Iezzi, T. Glass and H. C. Dorn, *Chem. Phys. Lett.*, 2003, **375**, 655–659.
11 T. Cai, L. S. Xu, M. R. Anderson, Z. X. Ge, T. M. Zuo, X. L. Wang, M. M. Olmstead, A. L. Balch, H. W. Gibson and H. C. Dorn, *J. Am. Chem. Soc.*, 2006, **128**, 8581–8589.
12 H. Kurihara, X. Lu, Y. Iiduka, N. Mizorogi, Z. Slanina, T. Tsuchiya, T. Akasaka and S. Nagase, *J. Am. Chem. Soc.*, 2011, **133**, 2382–2385.
13 H. Kurihara, X. Lu, Y. Iiduka, H. Nikawa, M. Hachiya, N. Mizorogi, Z. Slanina, T. Tsuchiya, S. Nagase and T. Akasaka, *Inorg. Chem.*, 2012, **51**, 746–750.

14 R. F. Curl, *Angew. Chem., Int. Ed.*, 1997, **36**, 1566–1576.
15 A. J. Stone and D. J. Wales, *Chem. Phys. Lett.*, 1986, **128**, 501–503.
16 M. Mulet-Gas, L. Abella, P. W. Dunk, A. Rodríguez-Fortea, H. W. Kroto and J. M. Poblet, *Chem. Sci.*, 2015, **6**, 675–686.
17 R. J. Cross and M. Saunders, *J. Am. Chem. Soc.*, 2005, **127**, 3044–3047.
18 Y. Zhang, K. B. Ghiassi, Q. Deng, N. A. Samoylova, M. M. Olmstead, A. L. Balch and A. A. Popov, *Angew. Chem., Int. Ed.*, 2015, **54**, 495–499.
19 C.-H. Chen, L. Abella, M. R. Cerón, M. A. Guerrero-Ayala, A. Rodríguez-Fortea, M. M. Olmstead, X. B. Powers, A. L. Balch, J. M. Poblet and L. Echegoyen, *J. Am. Chem. Soc.*, 2016, **138**, 13030–13037.
20 M. Yamada, H. Kurihara, M. Suzuki, J. D. Guo, M. Waelchli, M. M. Olmstead, A. L. Balch, S. Nagase, Y. Maeda, T. Hasegawa, X. Lu and T. Akasaka, *J. Am. Chem. Soc.*, 2014, **136**, 7611–7614.
21 M. M. Olmstead, H. M. Lee, J. C. Duchamp, S. Stevenson, D. Marciu, H. C. Dorn and A. L. Balch, *Angew. Chem., Int. Ed.*, 2003, **115**, 928–931.
22 N. Chen, M. Mulet-Gas, Y. Y. Li, R. E. Stene, C. W. Atherton, A. Rodriguez-Fortea, J. M. Poblet and L. Echegoyen, *Chem. Sci.*, 2013, **4**, 180–186.
23 B. Q. Mercado, C. M. Beavers, M. M. Olmstead, M. N. Chaur, K. Walker, B. C. Holloway, L. Echegoyen and A. L. Balch, *J. Am. Chem. Soc.*, 2008, **130**, 7854–7855.
24 X. Lu, H. Nikawa, T. Nakahodo, T. Tsuchiya, M. O. Ishitsuka, Y. Maeda, T. Akasaka, M. Toki, H. Sawa, Z. Slanina, N. Mizorogi and S. Nagase, *J. Am. Chem. Soc.*, 2008, **130**, 9129–9136.
25 T. Wakahara, H. Nikawa, T. Kikuchi, T. Nakahodo, G. M. A. Rahman, T. Tsuchiya, Y. Maeda, T. Akasaka, K. Yoza, E. Horn, K. Yamamoto, N. Mizorogi, Z. Slanina and S. Nagase, *J. Am. Chem. Soc.*, 2006, **128**, 14228–14229.
26 J. Zhang, F. L. Bowles, D. W. Bearden, W. K. Ray, T. Fuhrer, Y. Ye, C. Dixon, K. Harich, R. F. Helm, M. M. Olmstead, A. L. Balch and H. C. Dorn, *Nat. Chem.*, 2013, **5**, 880–885.
27 P. A. Troshin, A. G. Avent, A. D. Darwish, N. Martsinovich, A. K. Abdulsada, J. M. Street and R. Taylor, *Science*, 2005, **309**, 278–281.
28 I. N. Ioffe, C. Chen, S. Yang, L. N. Sidorov, E. Kemnitz and S. I. Troyanov, *Angew. Chem., Int. Ed.*, 2010, **49**, 4784–4787.
29 S. Yang, S. Wang, E. Kemnitz and S. I. Troyanov, *Angew. Chem., Int. Ed.*, 2014, **53**, 2460–2463.
30 B. Q. Mercado, N. Chen, A. Rodríguez-Fortea, M. A. Mackey, S. Stevenson, L. Echegoyen, J. M. Poblet, M. M. Olmstead and A. L. Balch, *J. Am. Chem. Soc.*, 2011, **133**, 6752–6760.
31 H. Yang, H. X. Jin, H. Y. Zhen, Z. M. Wang, Z. Y. Liu, C. M. Beavers, B. Q. Mercado, M. M. Olmstead and A. L. Balch, *J. Am. Chem. Soc.*, 2011, **133**, 6299–6306.
32 Y. Hao, Q. Tang, X. Li, M. Zhang, Y. Wan, L. Feng, N. Chen, Z. Slanina, L. Adamowicz and F. Uhlík, *Inorg. Chem.*, 2016, **55**, 11354–11361.
33 W. Cai, F.-F. Li, L. Bao, Y. Xie and X. Lu, *J. Am. Chem. Soc.*, 2016, **138**, 6670–6675.
34 P. Kuran, M. Krause, A. Bartl and L. Dunsch, *Chem. Phys. Lett.*, 1998, **292**, 580–586.
35 T. Inoue, T. Tomiyama, T. Sugai, T. Okazaki, T. Suematsu, N. Fujii, H. Utsumi, K. Nojima and H. Shinohara, *J. Phys. Chem. B*, 2004, **108**, 7573–7579.
36 H. Yang, H. X. Jin, B. Hong, Z. Y. Liu, C. M. Beavers, H. Y. Zhen, Z. M. Wang, B. Q. Mercado, M. M. Olmstead and A. L. Balch, *J. Am. Chem. Soc.*, 2011, **133**, 16911–16919.
37 H. Yang, C. Lu, Z. Liu, H. Jin, Y. Che, M. M. Olmstead and A. L. Balch, *J. Am. Chem. Soc.*, 2008, **130**, 17296–17300.
38 S. Zhao, P. Zhao, W. Cai, L. Bao, M. Chen, Y. Xie, X. Zhao and X. Lu, *J. Am. Chem. Soc.*, 2017, **139**, 4724–4728.
39 F. Melin, M. N. Chaur, S. Engmann, B. Elliott, A. Kumbhar, A. J. Athans and L. Echegoyen, *Angew. Chem., Int. Ed.*, 2007, **46**, 9032–9035.
40 M. N. Chaur, F. Melin, J. Ashby, B. Elliott, A. Kumbhar, A. M. Rao and L. Echegoyen, *Chem.–Eur. J.*, 2008, **14**, 8213–8219.
41 G. M. Sheldrick, *Acta Crystallogr., Sect. A: Found. Crystallogr.*, 2008, **64**, 112–122.